q dependence of the central peak in the inelastic-neutron-scattering spectrum of $SrTiO_3$

G. Shirane, R. A. Cowley,* M. Matsuda,† and S. M. Shapiro
Brookhaven National Laboratory, Upton, New York 11973
(Received 26 May 1993)

The recent discovery, by high-resolution x-ray-diffraction measurements, of two length scales in $SrTiO_3$ motivated a reinvestigation by neutron scattering of the soft phonon and associated central peak above the zone-boundary structural-phase-transition temperature ($T_c=99.5$ K). The central peak has an anisotropic q width which is determined by the anisotropy of the slopes of the dispersion curves. The correlation length derived from the energy-integrated intensities of the phonon and the central peak agree well with the short length scale measured in the x-ray studies. The sharp component, corresponding to the long length scale observed in the x-ray experiment just above T_c, is absent in the neutron-scattering measurement. Since the neutron experiment probes the total sample volume, the absence of the narrow component supports the view that it originates in the near-surface region of the crystal.

I. INTRODUCTION

The soft-mode theory of structural phase transitions is over 30 years old[1] and has been extraordinarily successful in describing a wide variety of structural phase transitions.[2] $SrTiO_3$ is a prototypical system because it exhibits both a zone-center soft mode, whose energy does not go to zero at finite temperatures,[3] and a zone-boundary (R point) phonon instability whose energy goes to zero as the temperature approaches T_c from above.[4] Later it was discovered that $SrTiO_3$ also exhibits an elastic central component associated with the zone-boundary phonon[5,6] and the intensity of this central peak diverges at T_c. This feature is called a "central component" because it is elastic and in an energy scan is at $\omega=0$, midway between the energy loss and gain peaks associated with the soft R-point phonon at $\omega=\pm\omega_\infty$. The central component is ubiquitous in the studies of structural phase transitions and is still not well understood.[6] Certain theories state it is dynamical due to anharmonic processes,[7] while other state it is related to defects in the sample.[8] The well-established elastic nature of the central peaks contradicts its dynamical origin and some evidence suggests a defect origin.[9]

The central peak in $SrTiO_3$ was studied in detail by Shapiro *et al.*[6] who interpreted the central component as a low-frequency resonance in the self-energy of the soft mode. Under certain conditions, the total inelastic neutron intensity can be written as the sum of a central peak part and a phonon part:

$$S(\mathbf{q},\omega)_{\rm tot}=S(\mathbf{q},\omega)_{\rm cent}+S(\mathbf{q},\omega)_{\rm phon}\ . \tag{1}$$

Integrating over energy, with $k_BT\gg\hbar\omega_\infty(T)$, Eq. (1) becomes

$$\frac{T}{\omega_0^2(\mathbf{q},T)}=\frac{T\delta^2}{\omega_0^2(\mathbf{q},T)\omega_\infty^2(\mathbf{q},T)}+\frac{T}{\omega_\infty^2(\mathbf{q},T)}\ , \tag{2}$$

where δ^2 is a measure of the coupling of the soft mode to some unspecified relaxing degree of freedom. The renormalized mode frequency $\omega_0(\mathbf{q},T)$ is given by

$$\omega_0^2(\mathbf{q},T)=\omega_\infty^2(\mathbf{q},T)-\delta^2(T)\ . \tag{3}$$

On cooling toward T_c, the soft-mode frequency decreases and the intensity of the sidebands increase as $T/\omega_\infty^2(\mathbf{q},T)$, but the central component increases even more rapidly, like $T/\omega_\infty^4(\mathbf{q},T)$ for $\omega_\infty^2\gg\delta^2$. The phase transition occurs when $\omega_0(T_c)=0$, but not when $\omega_\infty=0$. At T_c, $\omega_\infty^2=\delta^2$ and is nonzero provided $\delta^2(T_c)$ is nonzero. Figure 1 summarizes some of the earlier results on $SrTiO_3$. In Fig. 1(a), a typical inelastic-neutron-scattering spectrum is shown with a phonon peak at $\omega=\omega_\infty$ and the intense central peak at $\omega=0$. Figures 1(b) and 1(c) show the temperature dependence of ω_∞^2, δ^2, and ω_0^2 as a function of temperature.[6]

Recently, several perovskites, $SrTiO_3$ (Refs. 10–12), $KMnF_3$ (Refs. 13,14), and $RbCaF_3$ (Ref. 15) were examined using high-resolution x-ray scattering The main experimental difference between the x-ray and neutron-scattering techniques is that in an x-ray experiment the incident energy is very high ($\sim$8 keV), so energy analysis is nearly impossible and energy integration is automatically performed in the experiment. In a neutron experiment, the incident energy is low ($\sim$15 meV) and energy analysis is eary to perform. Consequently, x-ray studies focus on measuring the momentum dependence of the response and neutron techniques can measure either the momenta or the energy spectra. In the recent x-ray experiments on the perovskites, q scans around the R point were performed and the spectrum displays two length scales[12] as shown in Fig. 1(d) for $SrTiO_3$. There is a sharp peak resting on top of a broader response. The inverse of the linewidths corresponds to a long and short correlation length, respectively. The broad response has Lorentzian character and exhibits an anisotropy in q space in that it is about $\sqrt{2}$ larger when measured along the [110] direction compared to the [001] direction. The narrow component, called quasi-Bragg peak, has a Lorentzian squared shape and is isotropic in $\mathbf{q}$ space. The obvious question to pose is: What is the relationship between the narrow, quasi-Bragg component observed in

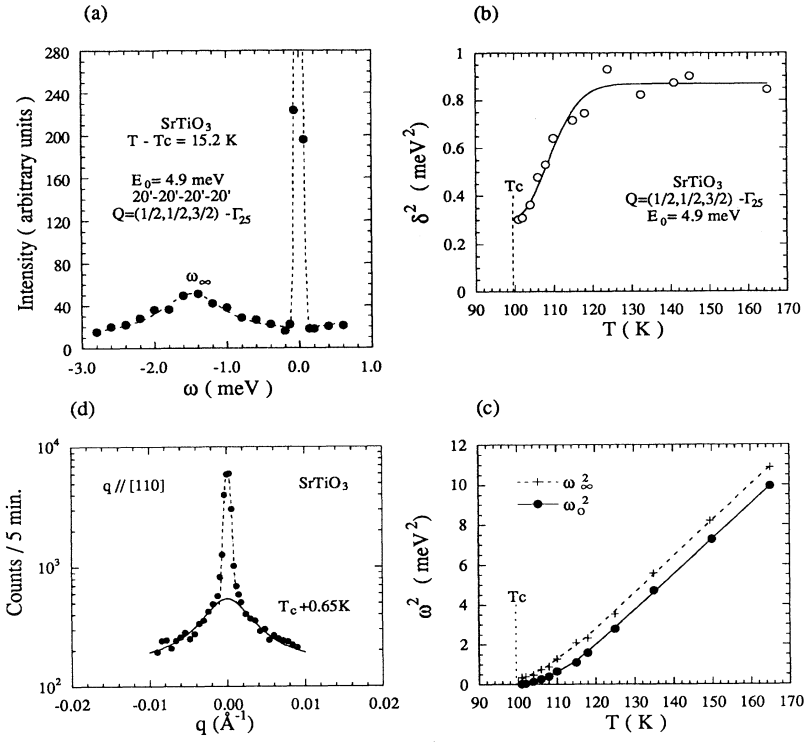

FIG. 1. Results of past studies on $SrTiO_3$: (a) Neutron inelastic spectrum showing peak due to phonon at $\omega=\omega_\infty$ and central peak at $\omega=0$; (b) δ^2 vs temperature (Ref. 6); (c) ω_∞^2 and ω_0^2 vs temperature (Ref. 6); (d) intermediate resolution x-ray diffraction spectrum showing the two length scales for $T_c+0.65$ K (Ref. 10).

the x-ray experiments and the central peak measured in the neutron studies? Cox and Cussen in their x-ray and neutron study[16] of $KMnF_3$ suggest that they are distinct, while Gibaud *et al.* claim that they are the same.[14] We attempt to answer this question by using neutrons to characterize the **q** dependence of the central peak in $SrTiO_3$ and compare it to the **q**-dependent x-ray measurements.

II. EXPERIMENT

We used the same $SrTiO_3$ crystal studied by Shapiro *et al.*[6] in 1972. It was grown by the top seeded method which yields an essentially strain-free crystal with an effective mosaic spread of 0.03° as determined by neutron diffraction and an actual mosaic of 15″ (0.004°) as determined by γ-ray diffraction.[17] The crystal is approximately cubic in shape with a volume ~ 1 cm^3. It has a brownish color and a transition temperature $T_c=99.5$ K. The lattice parameter at room temperature is 3.91 Å. The neutron-diffraction experiments were carried out at Brookhaven's high-flux beam reactor on the H-8 and H-7 triple-axis instruments. A variety of instrumental resolutions were used and Table I gives the values of the resolution for the various configurations and compares this with the reported x-ray resolution. It can be seen that in the best case, the neutron experimental resolution was within a factor of 3 of the x-ray experiment.

III. COMPARISON OF THE NEUTRON AND THE X-RAY RESULTS

Before comparing the present neutron results with the x-ray studies it is necessary to write the energy-integrated

TABLE I. Comparison of resolution width full width at half maximum (FWHM) in Å^{-1} for the x-ray experiments and the present neutron experiments on $SrTiO_3$.

	[100]	[011]	Vertical
X ray			
Andrews (Ref. 10) Intermediate resolution	0.0015	0.01	0.1–0.15
High resolution	0.001	0.001	0.1–0.15
McMorrow *et al.* (Ref. 12)	0.0012	0.0018	0.07
Nelmes *et al.* (Ref. 11)	0.0013	0.001	
Neutrons (10 min collimation) at $Q=(1.5,0.5,0.5)$			
$E_i=14.7$ meV	0.007	0.004	0.08
$E_i=5.0$ meV	0.004	0.004	0.06
$E_i=4.4$ meV	0.003	0.004	0.05

intensities given in Eq. (2) explicitly in its **q**-dependent form. The soft-mode frequency $\omega_\infty^2(\mathbf{q},T)$ has a dispersion which depends on the direction in the crystal. It can be written as

$$\omega_\infty^2(\mathbf{q},T)=\omega_\infty^2(0,T)+\alpha_q q^2 , \tag{4}$$

where $\omega_\infty^2(0,T)$ is the temperature-dependent frequency of the gap at the R point, taken as $q=0$, and α_q is the slope of the dispersion curve which depends upon the direction in the crystal. The lattice dynamics of $SrTiO_3$ have been extensively studied in the past and the phonon behavior is well known.[3,18] Figure 2 shows measurements of the soft-mode frequency along the [100] direction. The value

$$\alpha_{[100]}=3158 \text{ meV}^2 \text{ Å}^2 \tag{5}$$

is in very close agreement with that measured by Shapiro *et al.*[6] ($\alpha_{[100]}=3200$ meV Å^2) and by Stirling[18] ($\alpha_{[100]}=3233$ meV Å^2). Also, as seen in Fig. 2, $\alpha_{[100]}$ is temperature independent over the range $100<T<200$ K. Over this temperature range, the gap frequency follows an approximate linear temperature dependence:

$$\omega_\infty^2(0,T)\approx 0.18(T-T_c) . \tag{6}$$

The integrated phonon intensity given in Eq. (2) can now be written as

$$I_\infty(\mathbf{q},T)=\frac{T}{\omega_\infty^2(0,T)+\alpha_q q^2}=\frac{T/\alpha_q}{\kappa_\infty^2+q^2} , \tag{7}$$

where the phonon inverse correlation length is

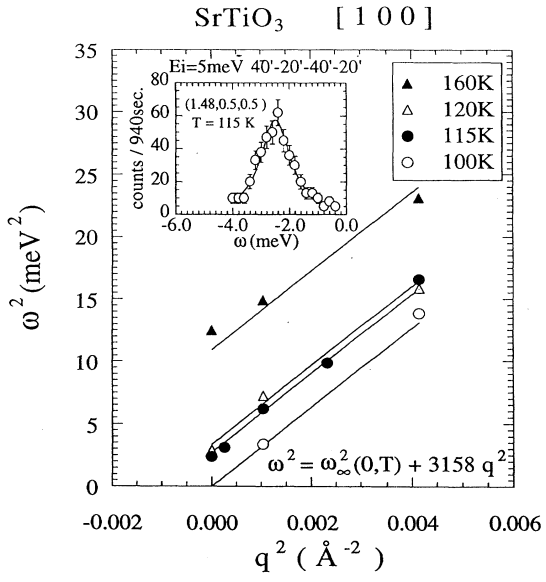

FIG. 2. The dispersion of the soft mode measured along the [100] direction at several temperatures. The temperature dependence of the soft mode at the R point ($q=0$) is $\omega_\infty^2(0,T)=0.18(T-T_c)$. The inset shows the inelastic spectrum.

$$\kappa_\infty^2=\frac{\omega_\infty^2(0,T)}{\alpha_q} . \tag{8}$$

Similarly, if we assume that the coupling constant δ^2 is **q** independent, we can define an inverse correlation length for the total scattering as

$$\kappa_0^2=\frac{\omega_0^2(0,T)}{\alpha_q} . \tag{9}$$

The difference between the two inverse correlation lengths is proportional to δ^2, namely,

$$\kappa_\infty^2-\kappa_0^2=\frac{\omega_\infty^2(0,T)-\omega_0^2(0,T)}{\alpha_q}=\frac{\delta^2}{\alpha_q} . \tag{10}$$

The form of the central peak can then be written as the difference of two Lorentzians:

$$\begin{aligned} I_{\text{cent}} &= \frac{T}{\alpha_q}\left[\frac{1}{\kappa_0^2+q^2}-\frac{1}{\kappa_\infty^2+q^2}\right] \\ &= \frac{T}{\alpha_q}\left[\frac{\kappa_\infty^2-\kappa_0^2}{(\kappa_0^2+q^2)(\kappa_\infty^2+q^2)}\right] \\ &= \frac{T}{(\alpha_q)^2}\left[\frac{\delta^2}{(\kappa_0^2+q^2)(\kappa_\infty^2+q^2)}\right] . \end{aligned} \tag{11}$$

At higher temperatures where $\omega_\infty^2 \gg \delta^2$ and consequently $\omega_0^2\approx\omega_\infty^2$, the central peak then has a Lorentzian squared line shape,

$$I_{\text{cent}}=\frac{T}{(\alpha_q)^2}\left[\frac{\delta^2}{(\kappa_0^2+q^2)^2}\right] . \tag{12}$$

The half width at half maximum (HWHM) of this central peak line shape is

$$\kappa_c=0.64\kappa_0 . \tag{13}$$

The temperature dependence of κ_c is a unique signature of the central peak and a quantity that can easily be verified experimentally. Close to T_c, the phonon frequency $\omega_\infty^2\approx\delta^2$, and the line shape of the central peak becomes Lorentzian and contains most of the response while $\kappa_c\approx\kappa_0$. From the temperature-dependent behavior of ω_∞^2, δ^2, and ω_0^2 given in Figs. 1(b) and 1(c), and the measured α_q, the quantities, κ_∞, κ_0, and κ_c can be calculated and are shown as solid lines for the [100] direction [Fig. 3(a)] and the [011] direction [Fig. 3(b)].

The high-resolution x-ray studies of $SrTiO_3$ show a narrow and broad peak [Fig. 1(d)] corresponding to long and short length scales, respectively.[12] The former was shown to have a Lorentzian squared shape with an inverse correlation length κ_{L2}, and the broader peak is Lorentzian with a HWHM of κ_{L1}. The dashed lines in Fig. 3 show the temperature dependence of these quantities as a measured by McMorrow *et al.*[12] κ_{L1} is very close to the value of κ_0 which implies that the broad component contains both the phonons and the central peak, i.e., is a measure of the total scattering given by Eqs. (1) and (2). This is expected since the x-ray measurement integrates over all energies. The width of the narrow,

quasi-Bragg component κ_{L2} is much smaller than any of the inverse correlation lengths derived from above and so is different from the central peak observed in the neutron scattering. It is an additional feature in the spectra whose origin is unclear. The rest of this paper is concerned with high-resolution neutron-scattering studies of the central peak to confirm the results presented above and to more fully characterize the central peak. We also report on a search for the quasi-Bragg peak using neutron scattering.

IV. CHARACTERIZATION OF THE CENTRAL PEAK

A. Integrated intensities

A major advantage of neutron scattering is the ability to do energy analysis and use energy to separate the central peak from the phonon. This is applicable over nearly the entire temperature region except near T_c, where the phonon energy becomes so small that it is difficult to distinguish the scattering of the central peak from that of the phonon. By performing energy scans at various momentum transfers and then integrating the observed intensity, the various κ's can be obtained using the formalism developed above. Unfortunately, this is very inefficient because the intensity of the inelastic scattering is weak and the accuracy is limited. Nevertheless, this process was performed at one temperature ($T=115$ K) and the q dependence of the integrated intensities of the phonon sidebands, the central peak, and the total scattering is shown in Fig. 4. Note that the integrated phonon intensities should include integration over both energy-gain and energy-loss parts of the spectra. In the experiment, only one peak was measured, and the intensity of the other calculated by applying the appropriate resolution and temperature correction and then added to the measured sideband. The κ values deduced are indicated in Fig. 4 and are shown as solid points in Fig. 3(a). The agreement with the κ's estimated from the measured values of ω_∞^2 and ω_0^2 above is good and indicates the validity of assuming that δ^2 is q independent. Note that κ_0 agrees very well with the broad linewidth measured by x rays which confirms that the x rays are measuring both the phonons and the central peak as expected from the lack of energy resolution in x-ray diffraction experiments.

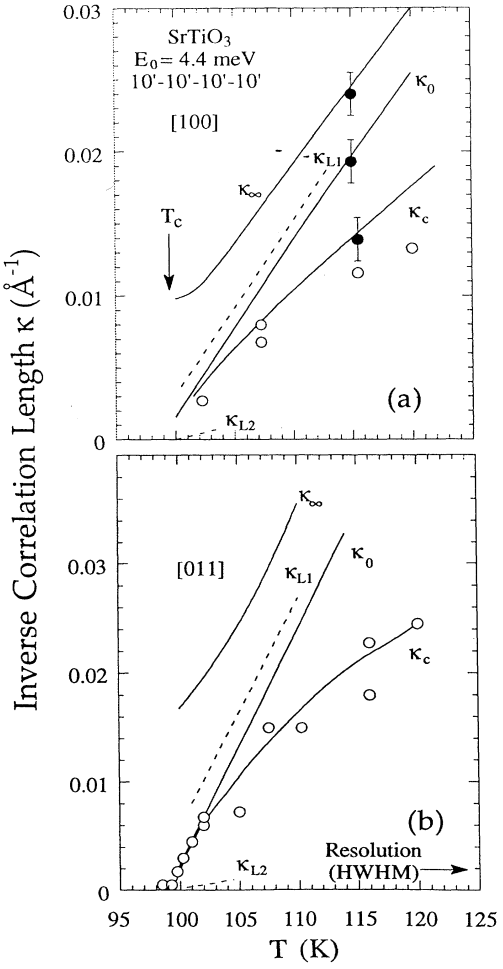

FIG. 3. (a) The inverse correlation lengths κ_∞, κ_0, κ_c along the [100] direction. The solid lines are determined from δ^2, ω_∞^2, and ω_0^2 from Ref. 6 and described in the text. The dashed lines are the two inverse correlation lengths determined from x-ray diffraction. The open circles are the current measurements for the central peak alone and the solid circles were obtained from Fig. 4; (b) the same as (a), only along the [011] direction.

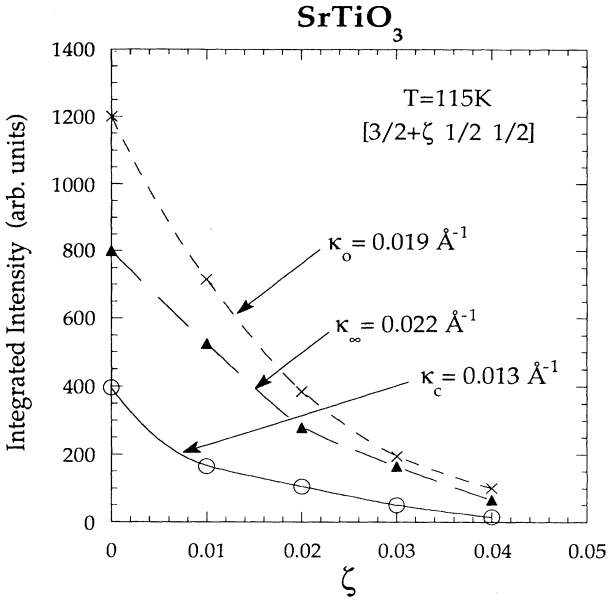

FIG. 4. The energy integrated intensities obtained from the inelastic measurements at each ζ value. The measured κ's are indicated in the figure.

B. Anisotropy

From Eqs. (9) and (13), κ_c is determined by the quantity α_q, which can be markedly different depending upon its direction. Figure 5(a) shows the dispersion curve measured at $T=115$ K along the [100] and the [011] direc-

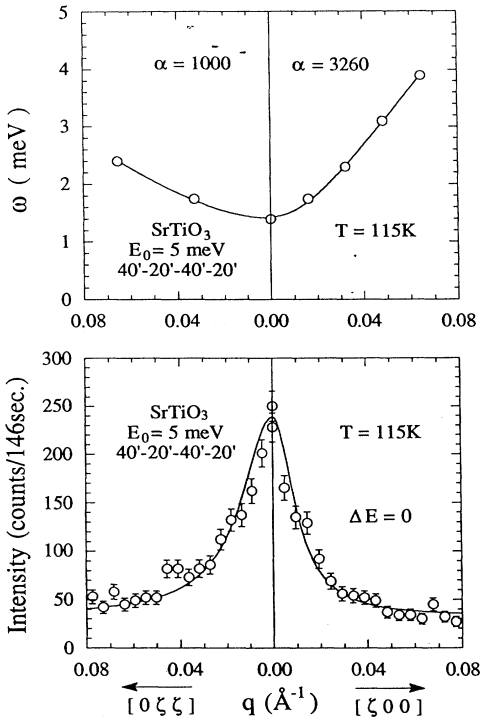

FIG. 5. Top: the measured dispersion of the soft mode about the R point along the [100] direction (right side) and the [011] direction (left side). The α values are slopes of $\omega(q)^2_\infty = \omega(0)^2_\infty + \alpha_q q^2$; Bottom: the q dependence of the central peak measured along the [100] (right side) and [011] (left side) directions.

tions. The ratio $(\alpha_{[100]}/\alpha_{[011]})^{1/2} = 1.8$ and this anisotropy should also occur in the width of the central peak κ_c for different wave vector directions. This is confirmed in Fig. 5(b) which compares the intensity of the central peak measured along the two different directions. The ratio of the widths is 1.8. Measurements were also made along the [013] direction where the ratio of the α's is different and these were consistent for the measured dispersion relations and widths of the central peak.

C. Temperature dependence

The earlier study of Shapiro *et al.*[6] showed that the central peak could be observed up to $T = 160$ K [see Fig. 1(b)]. In the present investigation we performed extensive q scans of the central peak alone along the [100] and [011] directions, measured at the (2.5,0.5,0.5) and (1.5,0.5,0.5) positions in reciprocal space. The spectra for scans along the [100] and [011] directions about (2.5,0.5,0.5) are shown for different temperatures in Fig. 6. The linewidth is larger for this direction since $\alpha_{[011]}$ is smaller, and, therefore, resolution corrections are less severe. The extracted values of κ_c are shown as open circles in Fig. 3(a) for the [100] direction and Fig. 3(b) for the [011] direction. The measurements agree very well with the calculations (solid line) given in Sec. III based on a q-independent δ^2 and the phonon behavior along the two different directions. It is quite clear that the central peak is distinct from the narrow peak, characterized by κ_{L2}, observed in the high-resolution x-ray experiment.

It is difficult to confirm the expected line shapes of the central peak. The major difference between Lorentzian and Lorentzian squared line shapes is in the wings. Far from T_c, the central component is expected to be Lorentzian squared but the intensity is too weak to distinguish between a Lorentzian and a Lorentzian squared line shape. The observed spectra can be fit equally well with either line shape. Close to T_c, the line shape should become more Lorentzian-like, but in this case it is too narrow and resolution effects become very important and preclude an accurate measure of the linewidth. The validity of the model is demonstrated by the agreement of the measured κ_c with the expected values, as shown in Fig. 3.

D. q dependence of coupling constant δ^2

Thus far we have assumed that δ^2 is q independent and it will be interesting to test this assumption. From Eq. (2)

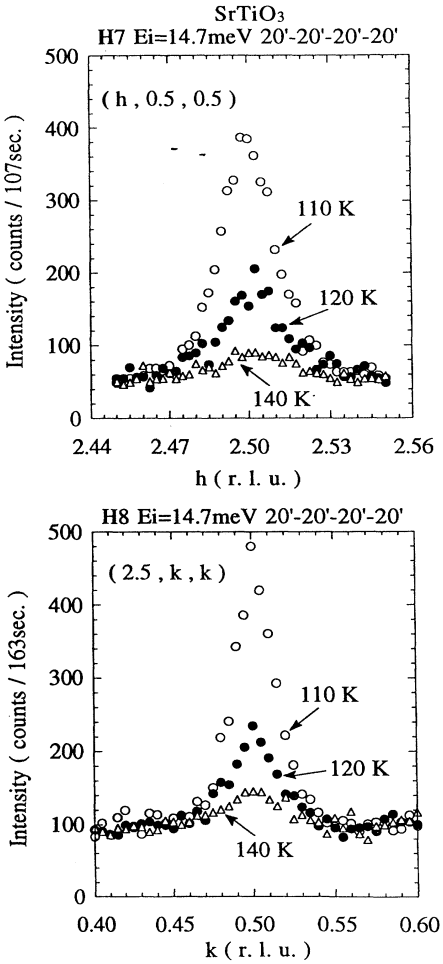

FIG. 6. Elastic scans along (top) [100] and (bottom) [011] directions in $SrTiO_3$ for several temperatures. For these temperatures only the central peak is measured in an elastic scan.

the ratio of the integrated central peak intensity to the integrated intensity of the phonon sidebands is

$$R \equiv \frac{I_{\text{cent}}}{I_{\text{phon}}} = \frac{\delta^2(\mathbf{q},T)}{\omega_0^2(\mathbf{q},T)} = \frac{\delta^2(\mathbf{q},T)}{\omega_\infty^2(\mathbf{q},T)-\delta^2(\mathbf{q},T)} , \quad (14)$$

and solving for $\delta^2(\mathbf{q},T)$, we obtain

$$\delta^2(\mathbf{q},T) = \frac{R}{R+1}\omega_\infty^2(\mathbf{q},T) . \quad (15)$$

Both R and $\omega_\infty^2(\mathbf{q},T)$ are directly measurable in a neutron experiment except in the region of small q near T_c, where the phonon and central peak overlap in energy. Figure 7 shows a plot of $\delta^2(\mathbf{q},T)$ vs q^2 measured along the [100] direction at $T=115$ K determined from Eq. (15). $\delta^2(\mathbf{q},T)$ increases for small q and then is nearly q independent. From the definition of $\omega_0^2(\mathbf{q},T)$ in Eq. (3) and the positive slope of $\delta^2(\mathbf{q},T)$ with q, we can write the q dependence of ω_0^2 as

$$\omega_0^2(\mathbf{q},T) = \omega_0^2(0,T) + \alpha'_{[100]} q^2 ,$$

where $\alpha'_{[100]}$ is smaller than $\alpha_{[100]}$ of Eq. (5). With this smaller α', κ_0 would increase slightly and give a closer agreement between the x-ray measurements of the broad component (κ_L) and the neutron determined κ_0 shown in Fig. 3.

One could, in principle, explain the narrow quasi-Bragg width κ_{L2} by a q dependence of δ^2. This would require α' to be much larger than α, which implies a *decrease* of δ^2 with q, which is opposite to our observations. In order to obtain the magnitude of $\kappa_{L2} \sim 0.003$ Å^{-1} at $T=115$ K, δ^2 would have to vary more steeply than the broad line shown in Fig. 7. This, clearly, is not observed and a q-dependent δ^2 cannot explain the narrow quasi-Bragg peak observed.

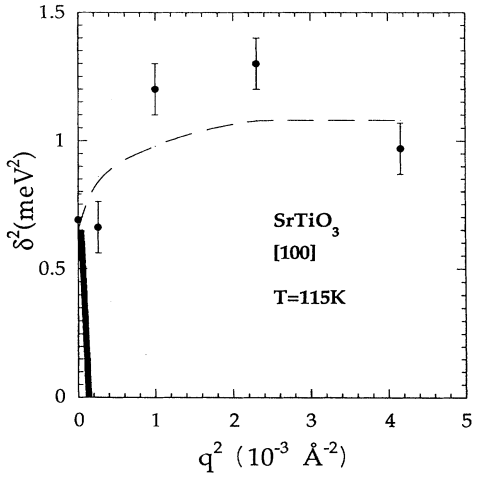

FIG. 7. δ^2 vs q^2 determined from the ratio of the integrated intensities of the central peak and the sidebands and ω_∞^2. [See Eqs. (14) and (15) in the text.] The dashed line is a guide to the eye. In order to explain the quasi-Bragg peak width, the q dependence of δ^2 would have varied more rapidly than shown by the bold line near $q=0$.

V. SEARCH FOR THE QUASI-BRAGG PEAK

We have shown that the central peak observed in the neutron-scattering experiment can be explained by coupling of the soft mode to a relaxational degree of freedom with a nearly q-independent coupling constant δ. The broad peak observed in the x-ray studies is due to the integrated intensities of the soft phonon and the central peak, which is distinct from the narrow peak observed in the x-ray studies. The question still remains as to the origin of the narrow quasi-Bragg peak with a reported Lorentzian squared line shape.

In order to distinguish the narrow component from the broad component, it is important to have the proper experimental resolution which, in this case, would be approximately the width of the narrow component. By using low-energy neutrons and narrow collimation, one can approach the resolution used in the x-ray experiment (Table I). Figure 8 shows q scans at zero-energy transfer through the R point along the [100] and [011] directions with an incident-neutron energy of 5.0 meV and 10′ collimation through the instrument. This resolution is still four to five times greater than the x-ray high-resolution study. Measurements were made at $T_c+0.5$ K and $T_c+2.5$ K. The curves are smooth with a single

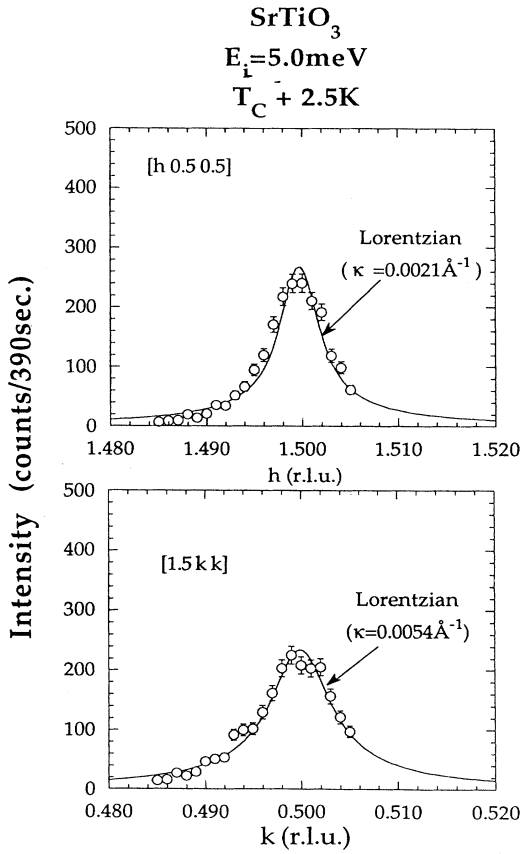

FIG. 8. Moderate resolution elastic-neutron-diffraction scans of the central peak along the [100] and the [011] direction about the 1/2(3,1,1) superlattice peak position for $T > T_c$. The solid lines are fits to a Lorentzian.

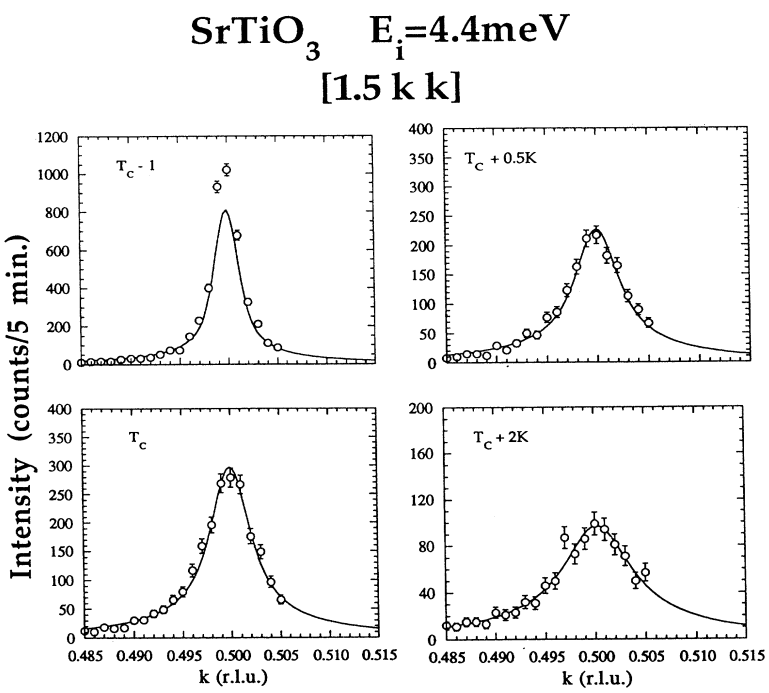

FIG. 9. High-resolution elastic-neutron-diffraction scans of the central peak along the [100] and the [011] direction about the 1/2(3,1,1) superlattice peak position. The solid lines are fits to a Lorentzian.

Lorentzian line shape. The width exhibits the expected anisotropy due to the different α_q along the two different directions and corresponds to the broad component seen in x rays. There is no sign of the sharp feature. In the next experiment, the incident energy was reduced to 4.4 meV and Table I shows that the resolution is improved to within a factor of 2 of the x-ray resolution. Scans were performed along the [011] direction since the central peak is broader than along the [100] direction and the sharp component would be easier to detect. The resolution and shape are accurately estimated by scanning through the low-temperature superlattice Bragg peak. The results are shown in Figs. 9 and 10 and no sharp component is visible in any of the profiles shown. Moreover, the central peak linewidth κ_c, obtained from the profiles, agrees well with the values calculated for the central peak in Fig. 3(b). The narrow, isotropic peak is absent.

The quantitative comparison with x-ray experiments requires detailed consideration of the effects of the resolution. Table I shows that with neutron energy of 4.4 meV, the resolution volume is five times larger than the high-resolution x-ray experiment of McMorrow *et al.*,[12] but has a similar volume of the intermediate resolution of Andrews' experiment as shown in Fig. 1(d). Thus, we conclude that the narrow peak present in the x-ray studies of $SrTiO_3$ is not present in the neutron experiment. Possible origins of this absence are: (i) The presence of the sharp quasi-Bragg component is very sample dependent and is not present in our exceptionally good single crystal. Studies on $RbCaF_4$ already showed that the presence of the sharp peak is sample dependent[15]; (ii) The neutrons are unable to see the quasi-Bragg component because it is only present on the outer, or near-surface area of the solid. Since x rays penetrate only a short distance

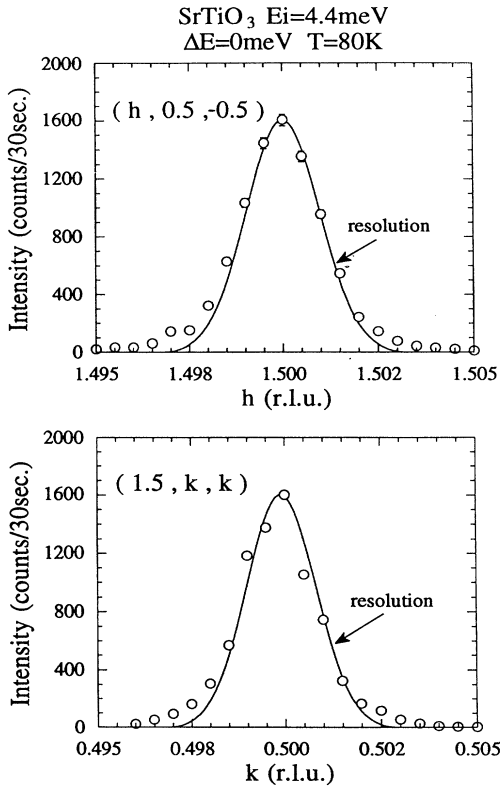

FIG. 10. High-resolution elastic-neutron-diffraction scans through the 1/2(3,1,1) superlattice Bragg peak along the [100] and [011] directions. The solid lines are the calculated resolution functions.

within the crystal they would have more sensitivity to this near-surface region than neutrons which detect the scattering from the entire volume of the sample. It is important to note that a recent study of the magnetic phase transition in holmium[19] and terbium[20] by x-ray and neutron diffraction also revealed the unexpected presence of two length scales above T_c (Ref. 10).

VI. SUMMARY

We have fully characterized the central peak in $SrTiO_3$ by performing high-resolution q scans above T_c. It was shown that the combined central peak and phonon scattering give rise to the anisotropic broad component observed in recent x-ray-diffraction experiments. A preliminary x-ray scattering experiment[21] on the same crystal of $SrTiO_3$ indicates the presence of only the sharp component in the diffraction pattern. The absence of the narrow component in the neutron experiment is consistent with the view that it originates in the near-surface region of the sample. This was shown to be the case for Tb in the most recent experiment,[20] where a particular scattering geometry was chosen.

ACKNOWLEDGMENTS

The authors appreciate the many discussions with our colleagues, including J. D. Axe, H. Chou, J. P. Hill, D. Gibbs, E. Lorenzo, and T. Thurston. We are also grateful to S. Andrews for providing us with unpublished x-ray-diffraction data. This work was carried out as part of the U.S.–Japan Cooperative Neutron-Scattering Program and was supported by the Division of Materials Science, U.S. Department of Energy, under Contract No. DE-AC02-76CH00016.

*Permanent address: Clarendon Laboratory, University of Oxford, Oxford OX1 3PU, England.

†Present address: The Institute of Physical and Chemical Research (RIKEN), Wako, Saitama 351-01, Japan.

[1]P. W. Anderson, in *Fizika Dielectrikov,* edited by G. I. Skanavi (Academy of Sciences, USSR, Mosscow, 1960); W. Cochran, Adv. Phys. **9**, 387 (1960).

[2]A. D. Bruce and R. A. Cowley, *Structural Phase Transitions* (Taylor & Francis, London, 1981); Adv. Phys. **29**, 219 (1980).

[3]R. A. Cowley, Phys. Rev. **134**, A981 (1964); Y. Yamada and G. Shirane, J. Phys. Soc. Jpn. **26**, 296 (1969).

[4]P. A. Fleury, J. F. Scott, and J. M. Worlock, Phys. Rev. Lett. **21**, 16 (1968); G. Shirane and Y. Yamada, Phys. Rev. **177**, 858 (1969); R. A. Cowley *et al.*, Solid State Commun. **7**, 181 (1969).

[5]T. Riste, E. J. Samuelsen, K. Otnes, and J. Feder, Solid State Commun. **9**, 1455 (1971).

[6]S. M. Shapiro, J. D. Axe, G. Shirane, and T. Riste, Phys. Rev. B **6**, 4332 (1972).

[7]R. A. Cowley and G. J. Coombs, J. Phys. C **6**, 143 (1973).

[8]B. I. Halperin and C. M. Varma, Phys. Rev. B **14**, 4030 (1976).

[9]J. B. Hastings, S. M. Shapiro, and B. C. Frazer, Phys. Rev. Lett. **40**, 237 (1978).

[10]S. R. Andrews, J. Phys. C **19**, 3721 (1986).

[11]R. J. Nelmes, P. D. Hatton, and H. Vass, Phys. Rev. Lett. **60**, 2172 (1980).

[12]D. F. McMorrow, N. Hamaya, S. Shimomura, Y. Fujii, S. Kishimoto, and H. Iwasaki, Solid State Commun. **76**, 443 (1990).

[13]U. J. Nicholls and R. A. Cowley, J. Phys. C **20**, 3417 (1987).

[14]A. Gibaud, H. You, S. M. Shapiro, and J. Y. Gesland, Phys. Rev. B **42**, 8255 (1990).

[15]T. W. Ryan, R. J. Nelmes, R. A. Cowley, and A. Gibaud, Phys. Rev. Lett. **56**, 2704 (1986); A. Gibaud, T. W. Ryan, and R. J. Nelmes, J. Phys. C **20**, 3833 (1987); A. Gibaud, R. A. Cowley, and P. W. Mitchell, J. Phys. C **20**, 3849 (1987).

[16]U. J. Cox, J. Phys. Condens. Matter **1**, 3565 (1989); U. J. Cox and L. D. Cussen, *ibid.* **1**, 3578 (1989).

[17]J. Schneider, J. E. Jørgensen, and G. Shirane, Phase Transitions **8**, 17 (1986).

[18]W. G. Stirling, J. Phys. C **5**, 2711 (1972).

[19]T. R. Thurston, G. Helgesen, D. Gibbs, J. P. Hill, B. D. Gaulin, and G. Shirane, Phys. Rev. Lett. **70**, 3151 (1993).

[20]P. M. Gehring, K. Hirota, C. F. Majkrzak, and G. Shirane, Phys. Rev. Lett. **71**, 1087 (1993).

[21]K. Hirota, J. P. Hill, S. M. Shapiro, and G. Shirane (unpublished).